Biofluidmechanics of Reproduction

Lisa J. Fauci[1] and Robert Dillon[2]

[1]Department of Mathematics, Tulane University, New Orleans, Louisiana 70118; email: fauci@tulane.edu;

[2]Department of Mathematics, Washington State University, Pullman, Washington 99164; email: dillon@math.wsu.edu

Annu. Rev. Fluid Mech. 2006. 38:371–94

The *Annual Review of Fluid Mechanics* is online at fluid.annualreviews.org

doi: 10.1146/annurev.fluid.37.061903.175725

0066-4189/06/0115-0371$20.00

Key Words

sperm motility, peristalsis, flagella, cilia, ovum transport

Abstract

Mammalian fertilization requires the coordinated activity of motile spermatozoa, muscular contractions of the uterus and oviduct, as well as ciliary beating. These elastic structures generate forces that drive fluid motion, but their configurations are, in turn, determined by the fluid dynamics. We review the basic fluid mechanical aspects of reproduction, including flagellar/ciliary beating and peristalsis. We report on recent biological studies that have shed light on the relative importance of the mechanical ingredients of reproduction. In particular, we examine sperm motility in the reproductive tract, ovum pickup and transport in the oviduct, as well as sperm-egg interactions. We review recent advances in understanding the internal mechanics of cilia and flagella, flagellar surface interaction, sperm motility in complex fluids, and the role of fluid dynamics in embryo transfer. We outline promising computational fluid dynamics frameworks that may be used to investigate these complex, fluid-structure interactions.

1. INTRODUCTION

There are no better illustrations of complex fluid-structure interactions than those that occur during the process of reproduction. Mammalian fertilization relies on the motility of spermatozoa, muscular contractions of the uterus and oviduct, as well as ciliary beating. Each of these generate forces that drive fluid motion, but at the same time the dynamic shapes of these elastic structures are determined by the fluid dynamics. The control of these force-generating mechanisms that cause the ovum and sperm to unite successfully is undoubtedly dictated by complex, physicochemical signaling. These chemicals diffuse in and are advected by the surrounding fluid. Therefore, the study of fluid dynamics is fundamental to the understanding of reproductive processes.

In this review, we provide an overview of classical work on ciliary and flagellar beating and peristalsis, all fundamental elements of the fluid dynamics of reproduction. However, despite considerable progress in modeling these elements individually, relatively few studies have examined the fluid dynamic coupling of these elements. We outline these modeling contributions, along with biological results that are elucidating the relative importance of the mechanical ingredients of reproduction. In particular, we examine sperm motility, ovum pickup and transport in the oviduct, as well as sperm-egg interactions. We also outline recent advances in computational biological fluid dynamics that promise to provide a framework for robust and accurate simulations of these complex, coupled dynamical systems.

2. SPERM-OVUM ENCOUNTER

Successful conception requires that a mature sperm arrive at the site of fertilization, the ampullar region of the fallopian tube (oviduct). The sperm must, therefore, progress from the insemination site through the cervix into the uterus, and from the uterus to the oviduct. In mammalian reproduction, the average number of sperm per ejaculate is tens to hundreds of millions. One would imagine, therefore, that just by sheer number, the likelihood of a successful sperm-egg encounter is incredibly high. In fact, only about one tenth of the sperm initially deposited ever reach the cervix, and only one tenth of those successfully penetrate the cervical mucus and reach the uterus. Only one tenth of those make it through the uterus to enter the oviducts (Eisenbach 2004). Once at the isthmus of the oviduct, sperm must progress through the narrow, mucus-containing lumen. Typically, they become attached to the mucosal epithelium and remain there until they have undergone capacitation, the physiological change that enables them to undergo the acrosome reaction that is essential for sperm penetration of the oocyte complex (Suarez 1996). This maturation is correlated with the timing of ovulation. Also acquired at this time is a motility pattern, termed hyperactivation (Ho & Suarez 2001a,b, 2003; Suarez 1996; Suarez & DeMott 1991; Yanagimachi 1970), in which the regular sinusoidal beating pattern of the flagellum is replaced by high-amplitude, asymmetric bending. (To compare regular, activated sperm waveforms with those of hyperactivated sperm, see **Figure 1**.) This vigorous beating may enable the sperm to detach from the mucosal epithelium and proceed

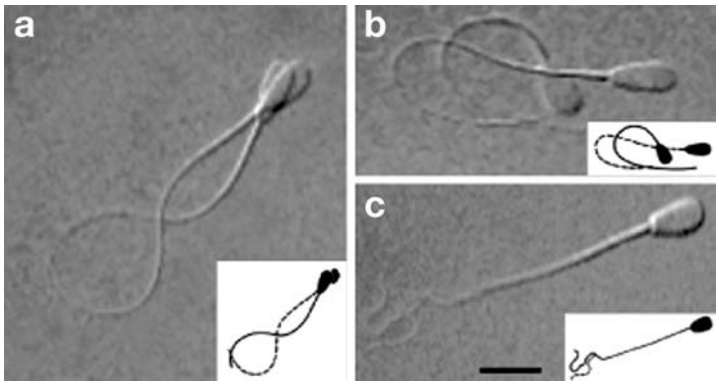

Figure 1

Videoimages of swimming patterns of bull spermatazoa. Each frame shows two images spaced 1/60 second apart. (*a*) Regular beat pattern of activated sperm. (*b*) Assymetric beat pattern of hyperactivated sperm. (*c*) Hyperactivated sperm in thick, viscoelastic solution. Reproduced from Ho & Suarez (2001a).

further up the oviduct toward the ampulla. The number of sperm that actually complete this tortuous journey and arrive at the oocyte for fertilization is very small, perhaps as few as one sperm per oocyte (Eisenbach 2004, Scott 2000). The guiding mechanisms that allow sperm to reach the fertilization site are fundamentally coupled to fluid mechanics.

It has long been established that in marine invertebrates, where fertilization occurs externally, sperm exhibit chemotaxis toward the female gamete (Eisenbach & Tur-Kaspa 1999). Chemotaxis of mammalian sperm was recently examined (Eisenbach 1999, 2004; Eisenbach & Tur-Kaspa 1999). Using various experimental setups, the accumulation of human sperm in vitro toward a possible attractant (e.g., follicular fluid) was measured. These include a bioassay in which a linear gradient of attractant is established through diffusion, and a choice assay in which spermatozoa choose between a well containing an attractant and a well containing a buffer as control. In addition, a directionality assay measures the tracks of individual sperm cells in a gradient of attractant. Eisenbach (2004) points out the importance of distinguishing between sperm accumulation due to chemotaxis, rather than accumulation due to speed enhancement or trapping. Examining the geometry of individual sperm tracks, although subjective, can provide visual evidence of chemotaxis, because chemotaxis can involve sharp directional changes in these tracks. Eisenbach & Tur-Kaspa (1999) present evidence that only a fraction of human sperm are chemotactically responsive to follicular fluid in vitro, and these are cells that have been capacitated. Because these are precisely those sperm that can undergo the acrosome reaction, this may be a selection mechanism that favors successful fertilization.

The identities of actual sperm chemoattractants in follicular or oviductal fluid, or in the oocyte cumulus complex (OCC) have not been established (Eisenbach 2004). Moreover, because there may be as few as one sperm arriving at the OCC, negative chemotaxis may be present, i.e., the OCC may send out a chemical signal preventing the arrival of other sperm (Eisenbach 2004). Further evidence for chemotaxis in mammalian reproduction, Eisenbach asserts, is given by Williams et al. (1993). Here although the number of sperm present in the nonovulating oviduct is approximately the same as the number present in the ovulating oviduct, the difference in spatial

distribution is significant—there are many more sperm present in the ampullar region of the ovulating oviduct, where fertilization occurs. Whether this is achieved due to sperm chemotaxis or the hormonally mediated mechanical activity of the oviductal muscles and cilia is not established. Eisenbach (2004) does point out that sperm chemotaxis is not the sole guiding mechanism for sperm-oocyte encounter, but may operate at short ranges. Unlike in vitro assays where linear attractant gradients can be established and maintained, it is not possible in vivo to maintain a linear gradient of attractant due to the muscular contractions and ciliary activity in the oviduct. Here a detailed study of the diffusion and advection of a chemical attractant within a fluid-filled, cilia-lined tube undergoing contractions may shed light on the mechanisms of sperm chemotaxis.

Another guidance mechanism, thermotaxis, was proposed by Bahat et al. (2003). In rabbit oviducts, there is a two-degree centigrade increase from the temperature in the isthmus to the temperature in the isthmic-ampullary junction, closer to the fertilization site. Bahat et al. (2003) used a directionality assay with two parallel wells separated by a partition maintained at different temperatures. As in the chemotaxis studies, only a fraction of the rabbit sperm were thermotactically responsive, and they were capacitated (Bahat et al. 2003). Bahat et al. speculate that sperm thermotaxis presents a long-range mechanism guiding the sperm-oocyte encounter.

Within minutes of mating, human sperm may be found within the oviduct (Scott 2000). Sperm swimming velocity cannot account for the long distance covered in such a short time. This rapid sperm transport is due to muscular contractions of the uterus (Kunz et al. 1997). Uterine peristalsis is essential for both sperm transport and fundal implantation of the embryo. Details of uterine peristalsis have been the study of experiments both in healthy females and females suffering from infertility (Eytan et al. 1999, Kunz et al. 1997, Leyendecker et al. 1996). The frequency and direction of peristaltic activity depend on the time of the cycle. Leyendecker et al. (1996) demonstrated that in healthy nonpregnant females, regular, symmetric peristaltic waves from the cervix to the fundus are present during the follicular phase. Using ultrasound, Eytan et al. (1999) measured the dynamics of the intrauterine fluid wall interface, as well as visualized the interior fluid flow. The boundary of the uterine cavity was determined by edge detection, and the dynamic properties of the mechanical wave motion were derived from changes in frame-to-frame geometry. During the proliferative phase of the ovulation cycle, symmetric peristaltic waves from the cervix to the fundus were observed. The amplitude of these waves decayed as they reached the fundus. The direction of these waves changed during menstruation (fundus to cervix), and the amplitude and frequency were significantly reduced. Leyendecker et al. (1996) measured uterine peristaltic activity in women with fertility problems due to endometriosis. During the late follicular phase, dysperistalsis was exhibited, where the peristaltic waves were arrhythmic and irregular. During the early and mid-follicular phase, these women exhibited hyperperistalsis, where the frequency of waves was double that of healthy women. This resulted in a dramatic increase in the transport of inert particles through the uterus to the oviducts as well as the peritoneal cavity. This enhanced transport mechanism for bacteria and other tissue fragments led Leyendecker et al. (1998) to conclude that hyperperistalsis is a mechanical cause of endometriosis.

Kunz et al. (1997) describe experiments aimed to study the dynamics of rapid sperm transport. Sperm-size albumin macrospheres were deposited vaginally, and their trajectories were measured in females using hysterosalpingoscintigraphy. More of these passive particles end up in the ovulating oviduct. Because these particles are nonmotile, Kunz et al. (1997) assert that chemotaxis does not play a role in rapid sperm transport.

3. SPERM MOTILITY

3.1. Classical Investigations of Flagellar Motion

Even within the low Reynolds number regime encountered by a motile spermatozoan, the coupled system of a viscous, incompressible fluid and a single flagellum or cilium—with a prescribed waveform—is difficult to analyze. In the past decades, the efforts to quantitatively describe the fluid dynamics of spermatozoa and ciliary propulsion have been very successful. Because inertial effects can be neglected, the linear Stokes flow assumption has been used to investigate the hydrodynamic consequences of flagellar undulations (Brennan & Winet 1977). The classical manuscript of G.I. Taylor (1951) initiated the fluid mechanical study of microorganism propulsion by analyzing the swimming of an infinitely long sheet undergoing small, constant, amplitude oscillations in a viscous fluid. The material points of the sheet did not progress to first order in amplitude; swimming was a second-order phenomenon. For a rich introduction to the biofluiddynamics of locomotion, see Lighthill (1975) and Childress (1981).

Subsequent to Taylor (1951), investigations of flagellar motility have been both analytical and computational. Resistive-force theory, initially developed by Gray & Hancock (1955), uses the linear Stokes flow assumption and describes the flagellum by a series of cylinders. The force on each small cylinder is computed by imagining that it is translating at its given orientation in the absense of neighboring cylinders. Central to this resistive force theory is the use of estimated resistance coefficients. Lighthill (1976) improved this theory by incorporating slender body approximations because the diameter of a flagellum is much smaller than its length. More detailed hydrodynamic analysis, such as refined slender body theory and boundary element methods, have produced excellent simulations of both two- and three-dimensional flagellar propulsion in an infinite fluid domain or in a domain with a fixed wall (Dresdner et al. 1980; Higdon 1979a,b; Phan-Thien et al. 1987). In all of these fluid dynamical models, the shape and the kinematics of the ciliary or flagellar beat was taken as given. However, the actual beatform is an emergent property of the coupled system consisting of the internal force generating mechanisms of the cilia or flagella, its passive elastic structure, and the external fluid dynamics.

3.2. Internal Ciliary and Flagellar Dynamics

The motion of eucaryotic cilia and flagella such as spermatozoa is governed by a mechanism that is entirely different from that of bacterial flagella. The bacterial

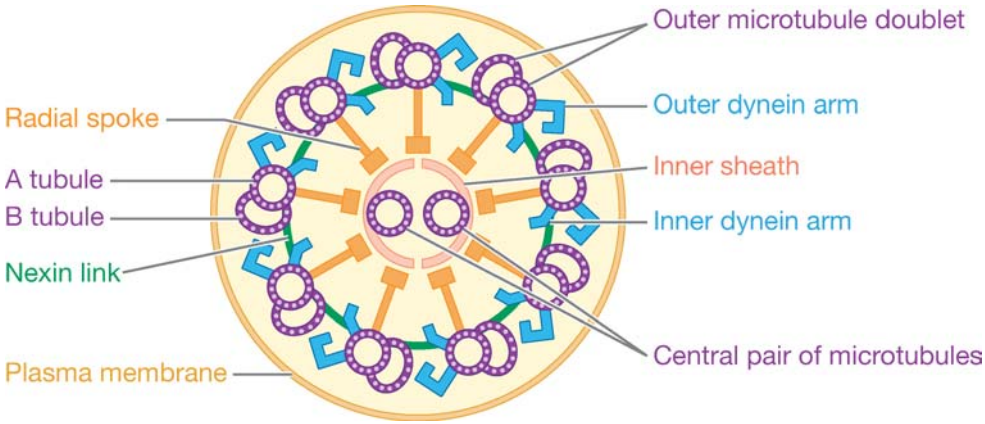

Figure 2

A schematic of a cross-section of a typical "9 + 2" eucaryotic axonemer. Reproduced from Cooper (2000).

flagellum is a rigid structure with a corkscrew shape and is rotated by a single motor (Berg 1975). In contrast, the eucaryotic flagellum has an elaborate internal structure, the axoneme, that is powered by dynein molecular motors distributed regularly along its length and circumference. Although the patterns of eucaryotic flagellar movement are distinct from those of ciliary movement, and flagella are typically much longer than cilia, their basic ultrastructure is identical. A schematic of a cross section of the typical "9 + 2" axoneme is shown in **Figure 2**. This cross section consists of a central pair of singlet microtubules surrounded by nine outer doublet microtubules and encased by the cell membrane (see Murase 1992, Witman 1990 for review). The nine outer doublets are connected by radial spokes to a sheath surrounding the central pair. In addition, the outer doublets are connected by protein structures, named nexin links, between adjacent pairs of doublets. The bending of the axoneme is caused by sliding between pairs of outer doublets. Active sliding is due to the unidirectional ATP-induced force generation of the dynein power stroke. Backward, passive sliding is due to the active sliding of other pairs of doublets within the axoneme. The radial spokes and central tubule couples are involved in the regulation of activity necessary in producing effective motion (Omoto 1991). The precise nature of the spatial and temporal control mechanisms regulating the various flagellar and ciliary beats is still unknown (Brokaw 2001).

Considerable interest has focused on understanding how the local force production of the dynein motors is translated into the controlled, regular beating of the global structure. An accurate mechanical model should include an explicit representation of the force generation and activation dynamics of the dynein molecular motors, and the forces due to the passive structure of the microtubules, nexin links, and radial arms. These forces should be coupled to the viscous hydrodynamics of the surrounding fluid.

Models for ciliary and flagellary motion based on a generalized resistive force theory have been developed and explored by several researchers. A derivation of this class of model is given by Hines & Blum (1978), and a comprehensive review is presented by Murase (1992). The model is expanded to include cross-bridge kinetics in Hines & Blum (1979). Brokaw (1971, 1972) proposed a model in which curvature controls the flagellar beat. This was expanded to include cross-bridge mechanics in Brokaw & Rintala (1975). Brokaw (2002) demonstrated that helical bending waves can be generated with a curvature control mechanism. Recently, Brokaw (2005) proposed an oscillatory dynein model for short flagella and nodal cilia. Oscillations have been observed in an experimental system consisting of a single microtubule overlayed onto an axonemal doublet with attached dyneins (Shinyoji 1998).

A model of ciliary beating that does include both internal bend-generating mechanics and accurate fluid dynamics was developed by Gueron & Levit-Gurevich (1998, 1999). In this work, digitized data from the beat pattern of a cilium of a *Paramecium* was used to calculate the parameters of an internal engine that depends only on the geometry of the cilium. This engine is used to generate force and is coupled to a hydrodynamic model. Realistic beat patterns emerge, and metachronism is exhibited in arrays of cilia (Gueron et al. 1997). In this model, the cilium is treated as a slender body, and there is no attempt to track the individual protein structures of the axoneme. A model that captures more of the detail of the 9+2 axoneme is presented by Gueron & Levit-Gurevich (2001).

Lindemann (1994a,b) developed the Geometric Clutch hypothesis for regulating flagellar and ciliary beats (for a review, see Lindemann 2004). He observed, in a wooden model of the axoneme, that the circular cross section of the axoneme was compressed in the plane of bending and proposed the term t-force to describe the resultant forces, which are transverse to the plane of bending in the axoneme. In the Geometric Clutch model, the direction of the t-force is reversed in active bending. The basic idea is that dynein attachment pulls together adjacent doublets and initiates a chain of attachment in the neighboring dyneins as the interdoublet spacing decreases. But the force generation of the attached dyneins creates sliding and bending. This active bending increases the transverse forces that pull the doublets apart and disengage the dyneins. This allows the dyneins on the opposite side of the axoneme to attach. The Geometric Clutch model has been explored through a series of papers (cf., Lindemann 1994a,b, 2003; Lindemann & Kanous 1995) that demonstrate that this hypothesis is consistent with many of the known experimental results for cilia and flagella. The computer models treat the axoneme as dynamic elastic linkages exerting force between longitudinal arrays of microtubules. Only a simple account of the hydrodynamics is included. Lindemann (2004) notes that acceptance of the Geometric Clutch hypothesis has been limited by the lack of experimental evidence for significant changes in interdoublet spacing during the flagellar and ciliary beats. However, recent advances by Mitchell (2003) in visualizing detailed geometric changes in the axoneme provide supporting evidence for this hypothesis.

A model for cilia and flagella, which incorporates discrete representations of the dynein arms, the passive elastic structure of the axoneme including the doublets and nexin links, was described in Dillon et al. (2003) and Dillon & Fauci (2000). This

model, based on the immersed boundary method (Peskin 1977, 2002), couples the internal force generation of the molecular motors through the passive elastic structure with the external fluid mechanics. Detailed geometric information is available, such as the spacing and shear between the microtubules, the local curvature of individual microtubules, and the stretching of the nexin links. In addition, the explicit representation of the dynein motors allows the flexibility to incorporate a variety of dynein activation theories. The structure of the two-dimensional model axoneme consists of a pair of microtubules. The microtubules are interconnected by horizontal links representing nexins and/or radial spokes. The dyneins are represented by dynamic, diagonal links connecting the two microtubules. Contraction of activated dyneins generates sliding between the two microtubules. One end of the dynein can attach, detach, and reattach to attachment sites on the microtubule. In cilia and flagella, the active sliding between adjacent pairs of microtubules can occur in only one direction. Thus, dyneins on different pairs of microtubules must be activated to produce a ciliary or flagellar beat. This is accomplished in the model by allowing two overlapping dynein configurations. The fluid is regarded as viscous and incompressible and the microtubule filaments that comprise the axoneme are elastic boundaries immersed in the fluid.

In Dillon & Fauci (2000) and Dillon et al. (2003), dynein activation is governed by a simple curvature control mechanism (Brokaw 1972). **Figure 3** shows a numerical simulation (R. Dillon, L. Fauci & C. Omoto, unpublished) of a swimming sperm. The upper panel shows a snapshot of the sperm and the fluid velocity field. The lower panel shows a detail of the axoneme. Dynein links (shown in red or blue) are activated after a lag time when the local curvature reaches a specified threshold. **Figure 4** shows simulation results of the ciliary waveform for two fluid viscosities (Dillon & Fauci 2000). In each panel, one complete cycle is depicted at equally spaced time intervals. Here the dyneins are activated uniformly during the effective stroke and from the base to the point of maximum curvature during the recovery stroke.

3.3. Sperm Motility in Complex Fluids

Spermatozoa encounter complex, non-Newtonian fluid environments as they progress through the female reproductive tract. In particular, the successful sperm must swim through cervical mucus, as well as eventually penetrate the cumulus layer of the oocyte complex. Passage through these gels undoubtedly involves a combination of enzymatic activity and hydrodynamic forces (Fulford et al. 1998). The difficult medium of cervical mucus may block abnormal sperm from entering the uterus, or may serve to "store" sperm until the time for fertilization is optimal (Katz & Berger 1980).

Figure 3

(*Upper*) A snapshot of a model sperm consisting of two microtubules and the surrounding fluid velocity field. Individual dynein motors governed by a curvature control mechanism cause flagellar bending. (*Lower*) Detail of the axonemal structure of the flagellum.

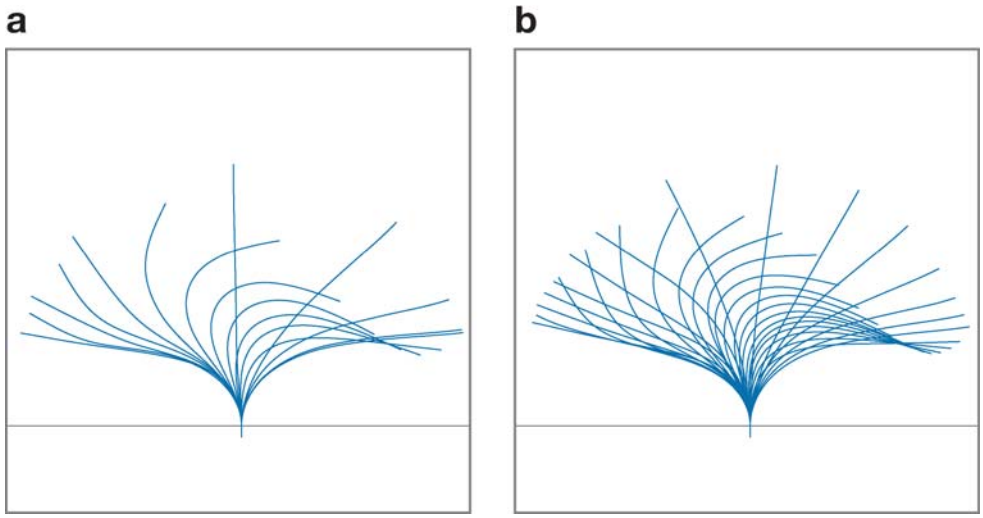

Figure 4

A ciliary waveform showing position of the cilium centerlines at a complete cycle at equally spaced time intervals until a complete cycle has been completed. The viscosity of the fluid was varied from panel to panel, with viscosities equal to: (*a*) 0.5, (*b*) 2.5 *cp*. In these simulations, dyneins were activated uniformly during the effective stroke and from the base to the point of maximum curvature during the recovery stroke. From Dillon & Fauci (2000).

Katz (1974) initiated the fluid dynamical analysis of sperm motility in narrow channels, such as a channel formed by aligned mucosal fibers. As in Taylor (1951), he considered an infinite sheet oscillating between two rigid walls. Using lubrication theory, it was established that for fixed wave kinematics, the swimming velocity of the sheet increased as the channel width decreased. Fauci & McDonald (1995) presented computations that agreed quantitatively with those of Katz (1974), but also varied the elastic properties of the channel walls. They found that the swimming velocities of the organisms bound by the channel walls decreased as the elasticity of the walls increased.

Katz et al. (1978) performed in vitro experiments that compared the swimming dynamics of human sperm in cervical mucus to those in a Newtonian fluid. In mucus, the flagellar bending was confined to the distal half of the flagellum. These bends exhibited lower amplitudes and wavelengths than those measured for flagella in Newtonian fluids. In addition, the swimming paths for sperm in mucus were much straighter than those in Newtonian fluids. Experiments were also performed on bovine sperm in cervical mucus in vitro (Katz et al. 1981), with particular attention to the difference between the dynamics of the "vanguard" sperm (the initial sperm entering the mucus) as compared to the followers. Although the beat kinematics were similar, the vanguard sperm had a significantly larger swimming velocity (35–44%) than its followers. This difference in velocity was enhanced for sperm near surfaces of the capillary tube. Here it is apparent that the elastic microstructure of the viscoelastic fluid is playing an important role in motility characteristics.

Previous analytical and computational models of flagellar motility assume Newtonian fluid dynamics. Recently, Fulford et al. (1998) presented a first step in modeling sperm motility in a viscoelastic fluid. Their model is based on a linear viscoelastic fluid coupled to a resistive force model for a flagellum beating with small-amplitude waves. In this simplified model, they demonstrate that for a fixed beat, there is no change in swimming velocity as compared to a Newtonian fluid model. However, the rate of work decreases as the elasticity of the medium increases for a Maxwell fluid. The development of refined models of flagellar motility in viscoelastic media that adopt either a continuum description of its elastic properties or explicitly represent the elastic microstructure presents an important avenue of investigation.

3.4. Hydrodynamic Sperm-Sperm and Sperm-Surface Interactions

There are many instances in the female reproductive tract where sperm are in close proximity to each other as well as to other surfaces. It has long been observed that when spermatozoa swim close together, they tend to beat in synchrony (Taylor 1951). In addition, groups of cilia exhibit metachronal waves, whereby neighboring cilia beat in synchrony, but a continuous phase difference results in the ciliary tips forming a traveling wave (Childress 1981). These phase-locking phenomena are due to hydrodynamic interactions. G.I. Taylor (1951) calculated that the mean energy dissipation between two waving infinite sheets is minimized when they beat in phase. However, the mechanism that achieved phase locking was not addressed. Using computational studies, Fauci (1990) demonstrated that neighboring waving sheets, initially beating with a phase lag, swim with different velocities until their relative position is phase locked. Fauci & McDonald (1995) also later demonstrated this for finite-length sperm.

An intriguing example of the hydrodynamic interaction of groups of sperm may be found in Moore et al. (2002). In small mammals, multiple matings cause sperm from different males to compete for fertilization within the reproductive tract of the same female. Spermatozoa from common wood mice exhibit cooperation and altruism in the following manner. The sperm heads of these mammals have a long apical hook whose end normally curls over and attaches to the ventral surface of the head. However, when a collection of individually swimming sperm from a given male are placed within a fertilization medium, within minutes their apical hooks become unhooked from the ventral side of their cell body and quickly hook onto the hooks or flagella of neighboring sperm. Motile clumps of tens to hundreds of cells are formed. These "sperm trains" swim significantly faster than individual sperm. This enhanced velocity is more pronounced in more viscous medium. In addition, Moore et al. (2002) showed that, when dispersed, most of the sperm in the sperm train underwent the acrosome reaction prematurely, and, therefore, cannot fertilize the oocyte themselves. There have not yet been any fluid dynamic investigations of these sperm trains.

Rothschild (1963) noted that the distribution of bull sperm in a drop of sperm suspension was not uniform, but accumulated near the surface of the microscope slide

and the coverslip. Rothschild attributed this to hydrodynamic interactions. Winet et al. (1984) studied the response of human spermatozoa to gravity, boundaries, and fluid shear. They found that the most influential stimulus was the boundary, or tube wall, at which the sperm accumulated. Fauci & McDonald (1995) performed two-dimensional fluid dynamic calculations of sperm swimming in a channel that also exhibited the tendency of a near wall to attract the organism.

Although the accumulation of sperm at surfaces is likely explained by hydrodynamic interactions with the surface, the detailed explanations may depend on factors such as the type of swimming motion (three-dimensional flagellar beat versus planar), or the asymmetry of the sperm head (Cosson et al. 2003, Wooley 2003). Cosson et al. (2003) points out that the attraction of sperm to surfaces is an efficient means for increasing sperm concentration in the vicinity of the egg. It would be interesting to investigate how aggregation propensity depends on different flagellar beat patterns, such as those observed during hyperactivation.

4. PERISTALSIS

4.1. Mathematical and Computational Models

Peristaltic pumping is a means of fluid transport that occurs when waves of contraction are passed along a tube containing liquid. It is a central mechanism of biological fluid transport and is responsible for rapid sperm transport from the uterus to the oviducts (Kunz et al. 1997), embryo transport to an implantation site in the uterus (Eytan et al. 2001a,b), and it contributes to ovum transport in the oviduct (Blake at al. 1983).

In past decades, many mathematical and computational models were developed to describe fluid flow in a tube undergoing peristalsis with prescribed wall motions. In earlier analytical studies, simplifying assumptions were made, including zero Reynolds number, small-amplitude oscillations, infinite wavelength, as well as symmetry of the channel (e.g., Burns & Parkes 1967, Jaffrin & Shapiro 1971). Subsequent studies have been less restrictive and have captured features such as finite wavelength, nonuniform channel geometry, and effects of finite-length channels (e.g., Eytan & Elad 1999, Fauci 1992, Li & Brasseur 1993, Pozrikidis 1987, Takabatake et al. 1988). A few models have been developed that capture the response of the tube walls to fluid forces, treating the walls as free boundaries (e.g., Griffiths 1989, Tang & Rankin 1993). In a recent study, a model of peristaltic pumping of a non-Newtonian fluid was proposed (Mernone et al. 2002).

4.2. Uterine Peristalsis and Embryo Transfer

Recently, there have been coordinated experimental, mathematical, and computational studies of uterine peristalsis (Eytan et al. 2001a,b, 2004; Eytan & Elad 1999; Yaniv et al. 2003). Because the Reynolds number of uterine peristalsis is about 10^{-3}, and the diameter of the uterine cavity is small, Eytan & Elad (1999) developed a Stokes flow model of peristalsis in a two-dimensional channel based on lubrication

theory. The channel walls oscillated sinusoidally, but with a phase shift. In a channel of uniform average cross section, they demonstrate that the transport phenomena are strongly affected by the phase shift between the walls. For a channel symmetric about its centerline, axial transport is optimized. This model was extended by Eytan et al. (2001b) to reflect the tapered geometry of the uterine cavity. These calculations demonstrate that axial velocity diminishes as the cross sections of the tube increase. Again, the phase shift between the walls has the largest effect on axial transport. Pressure gradients along the channel acting against the mechanical wave were applied. In some cases this caused reflux, where particles were transported in the direction opposite to the wave direction. This reflux was more pronounced in asymmetric peristaltic oscillations.

Embryo transfer is the last stage of in vitro fertilization, where the embryo is placed in the uterine cavity by means of a catheter. Although the success rate of sperm-egg fusion to form an embryo in the laboratory is greater than 90%, the overall rate of a successful birth is less than 25% (Yaniv et al. 2003). This may be due to implantation failure. In in vivo reproduction, the embryo is transported from the oviduct to the uterus and remains in the uterus for 3–4 days until it is transported by means of cervix-to-fundus myometrial contractions to an implantation site at the fundus (the upper part of the uterus). Understanding how the mechanics of the embryo transfer procedure couple with the fluid mechanics of uterine peristalsis may lead to improved procedures.

Eytan et al. (2001a) assert that the fluid mechanical phenomenon of reflux is the cause of unsuccessful embryo implantation in women who suffer from hydrosalpinx, a tubal pathology that causes buildup of fluid in the oviduct. This increases tubal pressure and results in an applied pressure gradient that acts against the peristaltic wave in the uterus that would otherwise transport the embryo to an appropriate implantation site at the fundus. Surgical removal of the oviduct with hydrosalpinx to improve implantation chances remains a controversial issue (Eytan et al. 2001a).

Yaniv et al. (2003) performed computational fluid dynamic simulations to study the coupling of a fluid-filled catheter inserted into a two-dimensional channel undergoing peristalsis. The computations were done using the software package FIDAP, with a moving mesh to capture the time-dependent geometry of the walls. They demonstrated that the speed of fluid injection from the catheter has a great effect on overall axial transport of particles within the channel. They conjecture that too high of an injection rate may lead to an ectopic pregnancy. In addition, Yaniv et al. (2003) examined the effect of the relative timing of initial injection with the phase of the peristaltic wave. This synchrony affects axial transport only at high injection rates.

The liquid medium within the catheter containing the embryos may affect embryo transfer and implantation. Air buffer zones are typically included in the catheter to prevent embryos from sticking to the catheter walls, and to prevent spillage (Eytan et al. 2004). Eytan et al. (2004) constructed a laboratory model of the uterine cavity and measured how the viscosity of the liquid medium, as well as the air volume fraction, affected the dynamic dispersal of the transferred volume of liquid. It was shown that air bubbles that form at the catheter tip inhibit dispersion of liquid from the catheter, and that better dispersion is achieved when the viscosity of the liquid

medium is close to that of the uterine fluid. In these experiments, the walls of the physical model of the uterine cavity were rigid.

It may be of critical importance in the study of embryo transport to develop models that account for the nonzero volume of the embryo, rather than treat it as a fluid marker. The embryo diameter at implantation is about 150μ, whereas the uterine channel diameter is on the order of 1000μ (Eytan & Elad 1999). There have been a couple of investigations of transport of solid particles by peristalsis. Hung & Brown (1976) performed experiments that examined the motion of a suspended particle due to the passage of a peristaltic wave and demonstrated that the velocity of the particle increased with particle diameter. Fauci (1992) performed numerical simulations of two-dimensional peristalsis where a circular solid particle is transported within a tube undergoing sinusoidal motion. These computations indicate that particle transport velocity increases geometrically as the particle diameter approaches the tube diameter.

5. OVUM PICKUP AND TRANSPORT

During ovulation, an OCC is released by the ovary and must be picked up by the fallopian tube or oviduct. The oocyte (ovum) is at the center of the OCC surrounded by two concentric layers. The innermost layer, the zona pellucida, is a glycoprotein layer that must be penetrated by the sperm for successful fertilization. Outermost is the cumulus layer, which contains cumulus cells bound together by an elastic matrix. The OCC is picked up by the infundibulum of the oviduct, whose external epithelial layer is covered by cilia that beat in the direction of the ostium, the entrance of the oviduct. (**Figure 5** shows a scanning electron micrograph of an OCC entering the ostium of the oviduct.) Using video microscopy, Talbot et al. (1999, 2003) demonstrate that the cilia-driven flow is strong enough to carry small particles, but is not sufficient to allow the OCC to be carried into the ostium. There must be adhesive interaction between the cumulus layer of the OCC and the ciliary tips in order for the OCC

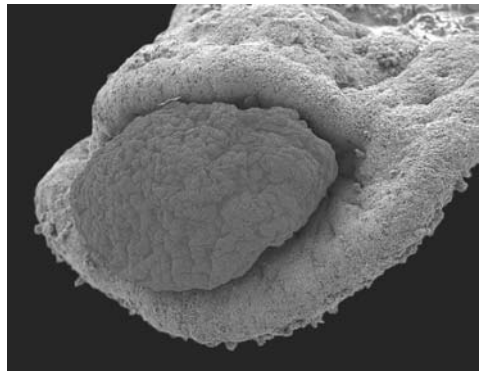

Figure 5

A scanning electron micrograph of an oocyte cumulus complex entering the ostium of the oviduct. We thank Professor P. Talbot, Department of Cell Biology and Neuroscience, University of California, Riverside for providing this image.

to make the necessary 180-degree turn to enter the oviductal lumen. The OCC attaches to the ciliary tips and glides over the surface of the infundibulum. Talbot et al. (1999, 2003) observe that when reaching the ostium, the OCC "churns" until the cumulus layer becomes compacted enough so that it may enter the ostium. There is an extension of the cells and matrix of the cumulus at the leading edge of the OCC that enters first into the ostium, while the back of the OCC still remains attached to the cilia. Eventually, this trailing edge breaks away from the ciliary tips, and the OCC enters the ostium. Because of the extension of the leading edge of the cumulus layer, the OCC that enters the oviduct has the oocyte positioned eccentrically in the OCC. Talbot et al. (1999) hypothesize that this could be a mechanism that enables easier sperm penetration.

The churning process described by Talbot et al. (1999) results in altering the mechanical properties of the elastic matrix. In fact, an OCC that had been retrieved from inside an oviduct, and hence had undergone this compactification, was unable to make the 180-degree turn into the ostium when placed on the exterior of the infundibulum. Talbot et al. (1999) also demonstrated negative effects of cigarette smoke on ovum pickup by the oviduct.

The combination of ciliary beating and adhesion of a viscoelastic matrix to the ciliary tips is essential for successful ovum pickup. Once the ovum enters the oviduct, it must be transported toward the uterus to a site where fertilization can occur, and then the fertilized ovum must be transported to the uterus. The oviduct is about 10-cm long and may be thought of as a tapered tube, with its widest section, the ampulla (.5−1.0 cm) nearest the ovary, and the smallest end, the isthmus (100−200μ diameter) nearest the uterus. The human ovum is about 150μ in diameter. The epithelium that lines the interior of the oviduct consists of ciliated and secretory cells. Fluid within the oviduct, and hence ovum transport, is driven by the action of these ciliated cells. In addition, the oviduct does undergo muscular contractions, which also contribute to ovum transport. The relative importance of these fluid dynamic mechanisms has been examined both experimentally and theoretically (e.g., Blake et al. 1983; Halbert et al. 1989, 1997; Osada et al. 1999; Verdugo et al. 1980).

Using treated rat oviducts, Halbert et al. (1989) studied the rate of transport of surrogate rat ova in situ. Using isoproteronal, smooth muscle activity was blocked. Isoproteronal did not have any effect on ciliary beat frequency. The rate of ovum transport (.03–.04 mm/sec) was unchanged in the noncontracting oviduct. They speculate that muscle contractility is, therefore, not necessary for fertility, but may provide a redundant mechanism for ovum transport. In addition, these muscular contractions cause undulatory movements of the ovum that may help to remove the outer cumulus mass and facilitate sperm penetration.

Osada et al. (1999) performed experiments to visualize fluid flow in the oviducts of rabbits. The fluid transport in the isthmic portion oscillates at one tenth of the oscillations observed in the ampulla portion. This suggests that transport in the isthmic portion is dominated by ciliary activity.

Tubal damage, perhaps due to infection, is a cause of infertility. Leng et al. (1998) demonstrated that decreased ciliation and low cilia beat frequency in surviving cilia are present in women with obstructive tubal infertility.

Kartegener's syndrome (KS) is a condition caused by defective cilia and is associated with respiratory problems, male infertility, and situs invertus (the reversal of the right-left positioning of internal organs). It had been thought that the cilia of KS patients are totally immotile. This assertion, coupled with the observation that four out of five female patients with KS are fertile, suggested that ciliary beating is not necessary for fertility (Blake et al. 1989). Halbert et al. (1997) performed biopsies of tubal mucosa of an infertile woman with KS and observed regions of ciliary activity. However, only a small proportion of the sites sampled showed ciliary activity, and there was significant spatial discontinuity. Moreover, the motility was dyskinetic with active cilia beating at a frequency of approximately one third of that of cilia found in normal mucosa. The discovery of active cilia, albeit dyskinetic, suggests that there is some level of ciliary activity that may be necessary for fertility. Finding a threshold for both spatial distribution of cilia and beat frequencies at which ovum transport can occur is a fluid mechanics issue that has not been addressed.

Verdugo et al. (1980) presented a stochastic model of ovum transport that was based on Langevin's diffusion equation. The ovum is assumed to undergo a one-dimensional random walk in a field of external force. This external force approximately captures ciliary beating and muscular contractions. Fluid effects were modeled by the inclusion of a frictional force on the ovum. This simple model predicted the leading role of ciliary activity in fast ovum transport in the ampulla. Verdugo et al. speculates that random muscular activity may be hormonally regulated to assist ovum transport in the uterine direction.

Blake et al. (1983) presented a fluid dynamic model of ovum transport in the oviduct that incorporates a representation of ciliary activity, muscular contractions, and applied pressure drop along the oviduct. They used lubrication theory to investigate ovum transport in the isthmus, where the ovum is in close contact with the vessel walls. A two-layer model was used to study flow in the ampulla. To study flow in the wider ampulla, an inner layer through which the ovum moves was coupled with an outer layer through which flow is assumed to be driven by pressure gradients only. The ciliary sublayer at the interface of the inner and outer layer is modeled by a distribution of volume forces. Analysis is based on balance of volume flow rates at cross sections of the oviduct. This simplified model of Blake et al. (1983) concluded that the ciliary beating can provide for the steady ovum transport, and that the muscular activity can result in highly oscillatory motion of the ovum. Also, it was hypothesized that the convoluted lumen of the oviduct allows leakback that may serve to reduce the pressure drop across the ovum in the narrow section of the oviduct where changes in pressure are great.

6. SPERM-EGG INTERACTION

For fertilization to occur, a sperm must successfully pass through the cumulus layer of the OCC and then adhere to and penetrate the zona pelludica (ZP), the glycoprotein layer that surrounds the oocyte (Talbot et al. 2003). In this process, the sperm undergoes the acrosomal reaction, where membranes of the front portion of the cell

body rupture and release various enzymes. The complex interplay between enzymatic activity and mechanical force that allows successful sperm penetration has been examined both theoretically and experimentally.

Green & Purves (1984), following Lighthill (1976), calculated that the hydrodynamic force exerted by a sperm flagellum would not be enough to break the covalent bonds of the ZP if it were a cross-linked structure. They concluded that the mechanical penetration alone would be possible only if the ZP behaved as a viscous gel. However, Green (1987) demonstrated that the ZP behaves as an elastic solid, and, therefore, mechanical force alone is insufficient for sperm penetration.

Baltz et al. (1988) performed coordinated experiments and hydrodynamic calculations [based on the resistive force of Gray & Hancock (1955)] that measured both thrust-derived force and torque-derived force of beating flagella. The pulling force of human sperm on pipettes was measured experimentally. This pulling force was consistently an order of magnitude smaller than that predicted by the thrust calculations that took as input the observed beat kinematics. However, the torque-derived force predicted was the same order of magnitude as the pulling force. Baltz et al. (1988) concluded that the pulling force on the pipette must be torque-derived. Adhesion between the sperm and the ZP occurs because they possess complementary receptor-ligand pairs. Using the hydrodynamic calculations, Baltz et al. (1988) argue that a single bond is sufficient to tether a sperm to the ZP. Once the sperm head is lying flat on the zona, acrosomal enzymes can dissolve an area of the ZP, and the sperm head can enter the penetration slit. (**Figure 6** shows a scanning electron micrograph of hamster sperm bound to a ZP.)

Stauss et al. (1995) showed experimentally that hyperactivation of hamster sperm facilitates the penetration of the ZP. The large-amplitude, asymmetric bends that are characteristic of hyperactivated motility were calculated by Drobnis et al. (1988) to generate increased force against surfaces. Suarez et al. (1991) measured the beat kinematics and swimming velocities of hyperactivated sperm in solutions with varying Ficoll concentrations. Using a modified resistive force theory that accounted for shear-thinning viscosity, they argue that hyperactivated sperm develop greater thrust at higher viscous loading.

There have been recent advances in experimentation that will enable more accurate modeling and, hence, a better understanding of the importance of fluid mechanical forces in sperm penetration of the ZP. Tollner et al. (2003) developed an experimental setup that, through the use of video microscopy, can observe the sequence of loose attachment to tight binding of macaque sperm on the ZP in vitro, as well as the acrosomal status of the sperm. Flagellar beat patterns at different stages of adhesion are measured. In addition, Sun et al. (2003) developed a micro-electro-mechanical system (MEMS) force sensor and measured the deformation of mouse oocytes and embryos due to an applied normal force. They reported that the puncturing force required for the oocyte was about one half of that required for the embryo. Fertilization changes the material properties of the ZP. Using a point-load mechanical model along with the measured data, they calculated the Youngs modulus of the mouse ZP as 17.9 kPa.

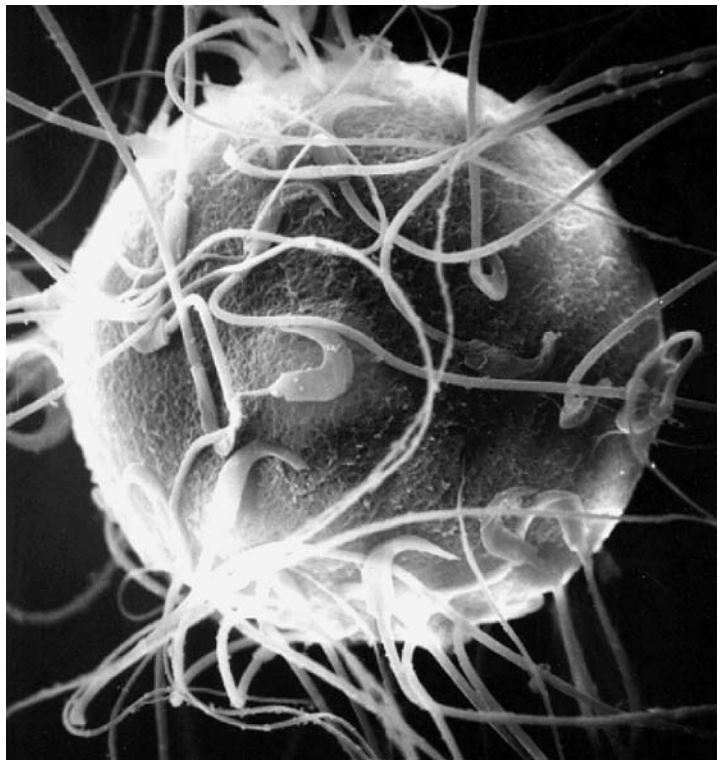

Figure 6

A scanning electron micrograph of hamster sperm bound to a zona pellucida. We thank Professor P. Talbot, Department of Cell Biology and Neuroscience, University of California, Riverside, for providing this image.

7. MODELING OF BIOFLUID-STRUCTURE INTERACTIONS

Computational simulation, in conjunction with laboratory experiments, can provide valuable insight into the biological fluid dynamic aspects of reproduction. Because the Reynolds number governing these flows is small, the boundary element method for Stokes flow has been used successfully in many instances (Pozrikidis 1992). Finite-element packages that allow the representation of complicated geometries have also been successful (e.g., Yaniv et al. 2003).

The immersed boundary method, originally developed by Peskin (1977) to model two-dimensional blood flow in the heart, provides a framework that can couple the elastic dynamics of flagella, cilia, and muscular walls with a viscous, incompressible fluid (for recent reviews, see Mittal & Iaccarino 2005 and Peskin 2002). These elastic objects are accounted for by suitable contributions to a force term in the fluid dynamics equations. The force of each object on the fluid is a Dirac delta-function layer of force supported only by the region of fluid that coincides with material points of the object. Once these forces on the fluid are accounted for, one can solve the fluid dynamics equations on a finite-difference or finite-element grid. Alternatively, for Stokes flow, one may use the grid-free method of regularized Stokeslets (Cortez

2001, Cortez et al. 2004b) that constructs the flow field due to a distribution of regularized forces supported by the immersed boundary. Note that the forces supported by these immersed boundaries may be chosen to reflect the biological properties of the structure, including constitutive properties of passive tissue, as well as active properties of muscle contraction or the action of molecular motors (Cortez et al. 2004a).

This immersed boundary framework has been used to study many problems in biological fluid dynamics, including three-dimensional blood flow in the heart (Peskin & McQueen 1989a,b), arteriolar flow in the kidney (Arthurs et al. 1998), aquatic animial locomotion (Cortez et al. 2004, Fauci & Peskin 1988), biofilm processes (Dillon et al. 1996), platelet aggregation (Fogelson et al. 2003), limb bud development (Dillon & Othmer 1999), and growth of the trophoblast layer in a human placenta (Rejniak et al. 2004). Studies directly related to the fluid dynamics of reproduction include models of ciliary and flagellar beating (Dillon et al. 2003, Dillon & Fauci 2000), interaction of flagella (Fauci 1990, Fauci & McDonald 1995), peristaltic pumping of solid particles (Fauci 1992), and three-dimensional helical swimming (Cortez et al. 2004b). In addition, Bottino (1998) demonstrated that the microstructure of a viscoelastic material can be successfully modeled within this framework.

8. CONCLUSION

The complex interplay of fluid mechanical phenomena that are central to the reproductive process presents a wealth of interesting, challenging, and biomedically important problems for investigation. In the last 50 years, there have been great advances in understanding (separately) the fundamental fluid mechanics of flagellar motility, ciliary beating, and peristalsis. The challenge now is to understand the fluid dynamic coupling of these mechanisms in realistic geometries. In addition, it is essential to capture the fluid-structure interactions that allow the configurations of the tube walls, cilia, and flagella to respond to fluid forces. Further advances in the study of the biofluidmechanics of reproduction will require refined models of flagellar motility in viscoelastic media, as well as multiscale models that couple the ATP-driven activation cycle of dynein motors in the axoneme with the external fluid dynamics. We await detailed models that examine the fluid dynamics of hyperactivated sperm in contact with oviductal epithelium or the zona pellucida of the oocyte cumulus complex. A better understanding of ovum transport, as well as embryo transfer in in vitro fertilization, will be achieved by models that treat the ovum or embryo as a solid object, rather than a fluid marker.

LITERATURE CITED

Arthurs KM, Moore LC, Peskin CS, Pitman EB, Layton HE. 1998. Modeling arteriolar flow and mass transport using the immersed boundary method. *J. Comp. Phys.* 147:402–40

Bahat A, Tur-Kaspa I, Gakamsky A, Giojalas L, Breitbart H, Eisenbach M. 2003. Thermotaxis of mammalian sperm cells: a potential navigation mechanism in the female genital tract. *Nature Med.* 9:149–50

Baltz JM, Katz DF, Cone RA. 1988. Mechanics of sperm-egg interaction at the zona pellucida. *Biophys. J.* 54:643–54
Berg HC. 1975. How bacteria swim. *Sci. Am.* 233:36–44
Blake JR, Vann PG, Winet H. 1983. A model of ovum transport. *J. Theor. Biol.* 102:145–66
Bottino D. 1998. Modeling viscoelastic networks and cell deformation in the context of the immersed boundary method. *J. Comp. Phys.* 147:86–113
Brennen C, Winet H. 1977. Fluid mechanics of propulsion by cilia and flagella. *Annu. Rev. Fluid Mech.* 9:339–98
Brokaw CJ. 1971. Bend propagation by a sliding filament model for flagella. *J. Exp. Biol.* 55:289–304
Brokaw CJ. 1972. Computer simulation of flagellar movement I. Demonstration of stable bend propagation and bend initiation by the sliding filament model. *Biophys. J.* 12:564–86
Brokaw CJ. 2001. Simulating the effects of fluid viscosity on the behavior of sperm flagella. *Math. Meth. Appl. Sci.* 24:1351–65
Brokaw CJ. 2002. Computer simulation of flagellar movement VIII: Coordination of dynein by local curvature control can generate helical bending waves. *Cell Motil. Cytoskelet.* 53:103–24
Brokaw CJ. 2005. Computer simulation of flagellar movement IX. Oscillation and symmetry breaking in a model for short flagella and nodal cilia. *Cell Motil. Cytoskelet.* 60:35–47
Brokaw CJ, Rintala D. 1975. Computer simulation of flagellar movement III. Models incorporating cross-bridge kinetics. *J. Mechanochem. Cell Motil.* 3:77–86
Burns JC, Parkes T. 1967. Peristaltic motion. *J. Fluid Mech.* 29:731–43
Childress S. 1981. *Mechanics of Swimming and Flying*. Cambridge, UK: Cambridge Univ. Press
Cooper GM. 2000. *The Cell: A Molecular Approach*, *Second Edition*. Sunderland, MA: Sinauer Assoc.
Cortez R. 2001. The method of regularized Stokeslets. *SIAM J. Sci. Comput.* 23:1204–25
Cortez R, Cowen N, Fauci L, Dillon R. 2004. Simulation of swimming organisms: coupling internal mechanics with external fluid dynamics. *Comp. Sci. & Eng.* 6:38–45
Cortez R, Fauci L, Medovikov A. 2005. The method of regularized stokeslets in three dimensions: analysis, validation, and application to helical swimming. *Phys. Fluids* 17:031504-1-14
Cosson J, Huitorel P, Gagnon C. 2003. How spermatozoa come to be confined to surfaces. *Cell Motil. Cytoskel.* 54:56–63
Dillon R, Fauci L. 2000. An integrative model of internal axoneme mechanics and external fluid dynamics in ciliary beating. *J. Theor. Biol.* 207:415–30
Dillon R, Fauci L, Fogelson A, Gaver D. 1996. Modeling biofilm processes using the immersed boundary method. *J. Comp. Phys.* 129:57–73
Dillon R, Fauci L, Omoto C. 2003. Mathematical modeling of axoneme mechanics and fluid dynamics in ciliary and sperm motility. *Dyn. Cont. Dis. & Imp. Sys.* 10:745–57

Dillon R, Othmer H. 1999. A mathematical model for the outgrowth and spatial patterning of the vertebrate limb bud. *J. Theor. Biol.* 197:295–330
Dresdner RD, Katz DF, Berger S. 1980. The propulsion by large amplitude waves of uniflagellar micro-organisms of finite length. *J. Fluid Mech.* 97:591–621
Drobnis E, Yudin A, Cherr G, Katz D. 1988. Hamster sperm penetration of the zona pellucida: kinematic analysis and mechanical implications. *Dev. Biol.* 130:311–23
Eisenbach M. 2004. *Chemotaxis*. London: Imperial College Press
Eisenbach M. 1999. Mammalian sperm chemotaxis and its association with capacitation. *Dev. Gen.* 25:87–94
Eisenbach M, Tur-Kaspa I. 1999. Do human eggs attract spermatozoa? *BioEssays* 21:203–10
Eytan O, Azem F, Gull I, Wolman I, Elad D, Jaffa AL. 2001. The mechanism of hydrosalpinx in embryo implantation. *Hum. Reprod.* 16:2662–67
Eytan O, Elad D. 1999. Analysis of intra-uterine fluid motion induced by uterine contractions. *Bull. Math. Biol.* 61:221–38
Eytan O, Elad D, Zaretsky U, Jaffa AL. 2004. A glance into the uterus during in vitro simulation of embryo transfer. *Hum. Reprod.* 19:562–69
Eytan O, Jaffa AL, Elad D. 2001. Peristaltic flow in a tapered channel: application to embryo transport within the uterine cavity. *Med. Eng. Phys.* 23:473–82
Eytan O, Jaffa AJ, Har-Toov J, Dalach E, Elad D. 1999. Dynamics of the intrauterine fluid-wall interface. *Ann. Biomed. Eng.* 27:372–79
Fauci L. 1990. Interaction of oscillating filaments - a computational study. *J. Comp. Phys.* 86:294–313
Fauci L. 1992. Peristaltic pumping of solid particles. *Comp. & Fluids* 21:583–98
Fauci L, McDonald A. 1994. Sperm motility in the presence of boundaries. *Bull. Math. Biol.* 57:679–99
Fauci L, Peskin CS. 1988. A computational model of aquatic animal locomotion. *J. Comp. Phys.* 77:85–108
Fogelson A, Kuharsky A, Yu H. 2003. Computational modeling of blood clotting: coagulation and three-dimensional platelet aggregation. In *Polymer and Cell Dynamics: Multicsale Modeling and Numerical Simulations*, ed. W Alt, M Chaplain, M Griebel, J Lenz. Basel: Birkhaeuser-Verlag
Fulford G, Katz DF, Powell R. 1998. Swimming of spermatozoa in a linear viscoelastic fluid. *Biorheology* 35:295–309
Gray J, Hancock G. 1955. The propulsion of sea-urchin spermatozoa. *J. Exp. Biol.* 32:802–14
Green DP. 1987. Mammalian sperm cannot penetrate the zona pellucida solely by force. *Exp. Cell Res.* 169:31–38
Green DP, Purves RD. 1984. Mechanical hypothesis of sperm penetration. *Biophys. J.* 45:659–62
Griffiths DJ. 1989. Flow of urine through the ureter: a collapsible, muscular tube undergoing peristalsis. *J. Biomech. Eng.-Trans. ASME* 111:206–11
Gueron S, Levit-Gurevich K. 1998. Computation of the internal forces in cilia: application to ciliary motion, the effects of viscosity, and cilia interactions. *Biophys. J.* 74:1658–76

Gueron S, Levit-Gurevich K. 1999. Energetic considerations of ciliary beating and the advantage of metachronal coordination. *Proc. Natl. Acad. Sci. USA* 96:12240–45

Gueron S, Levit-Gurevich K. 2001. A three-dimensional model for ciliary motion based on the internal 9+2 structure. *Proc. R. Soc. London Ser. B* 268:599–607

Gueron S, Levi-Gurevich K, Liron N, Blum JJ. 1997. Cilia internal mechanism and metachronal coordination as the result of hydrodynamic coupling. *Proc. Natl. Acad. Sci. USA* 94:6001–6

Halbert SA, Becker DR, Szal SE. 1989. Ovum transport in the rat oviductal ampulla in the absence of muscle contractility. *Biol. Reprod.* 40:1131–36

Halbert SA, Patton DL, Zarutskie PW, Soules MR. 1997. Function and structure of cilia in the fallopian tube of an infertile woman with Kartagener's syndrome. *Hum. Reprod.* 12:55–58

Higdon JJL. 1979. A hydrodynamic analysis of flagellar propulsion. *J. Fluid Mech.* 90:685–711

Higdon JJL. 1979. The hydrodynamics analysis of flagellar propulsion: helical waves. *J. Fluid Mech.* 94:331–51

Hines M, Blum JJ. 1978. Bend propagation in flagella I. Derivation of equations of motion and their simulation. *Biophys. J.* 23:41–57

Hines M, Blum JJ. 1979. Bend propagation in flagella II. Incorporating of dynein cross-bridge kinetics into the equations of motion. *Biophys. J* 25:421–42

Ho H, Suarez S. 2001. Hyperactivation of mammalian spermatozoa: function and regulation. *Reproduction* 122:519–26

Ho H, Suarez S. 2001. An inositol 1,4,5-Triphosphate receptor-gated intracellular Ca^{2+} store is involved in regulating sperm hyperactivated motility. *Biol. Reprod.* 65:1606–15

Ho H, Suarez S. 2003. Characterization of the intracellular calcium store at the base of the sperm flagellum that regulates hyperactivated motility. *Biol. Reprod.* 68:1590–96

Hung TK, Brown TD. 1976. Solid-particle motion in two-dimensional peristaltic flows. *J. Fluid Mech.* 73:77–96

Jaffrin M, Shapiro A. 1971. Peristaltic pumping. *Annu. Rev. Fluid Mech.* 3:13–36

Katz DF. 1974. On the propulsion of micro-organisms near solid boundaries. *J. Fluid Mech.* 64:33–49

Katz DF, Berger SA. 1980. Flagellar propulsion of human sperm in cervical mucus. *Biorheology* 17:169–75

Katz DF, Bloom TD, BonDurant RH. 1981. Movement of bull spermatozoa in cervical mucus. *Biol. Reprod.* 25:931–37

Katz DF, Mills RN, Pritchett TR. 1978. The movement of human spermatozoa in cervical mucus. *J. Reprod. Fert.* 53:259–65

Kunz G, Beil D, Deiniger H, Einspanier A, Mall G, Leyendecker G. 1997. The uterine peristaltic pump. Normal and impeded sperm transport within the female genital tract. *Adv. Exp. Med. Biol.* 424:267–77

Leng Z, Moore DE, Mueller BA, Critchlow CW, Patton DL, et al. 1998. Characterization of ciliary activity in distal Fallopian tube biopsies of women with obstructive tubal infertility. *Hum. Reprod.* 11:3121–27

Leyendecker G, Kunz G, Wildt L, Beil D, Deininger H. 1996. Uterine hyperperistalsis and dysperistalsis as dysfunctions of the mechanism of rapid sperm transport in patients with endometriosis and infertility. *Hum. Reprod.* 11:1542–51
Li MJ, Brasseur JG. 1993. Nonsteady peristaltic transport in finite-length tubes. *J. Fluid Mech.* 248:129–51
Lighthill JL. 1975. Mathematical biofluiddynamics. In *Regional Conference Series in Applied Math*, Vol. 17. Philadelphia: SIAM
Lighthill JL. 1976. Flagellar hydrodynamics. *SIAM Rev.* 18:161–230
Lindemann C. 1994. A model of flagellar and ciliary functioning which uses the forces traverse to the axoneme as the regulator of dynein activation. *Cell Motil. Cytoskelet.* 29:141–54
Lindemann C. 1994. A geometric clutch hypothesis to explain oscillations of the axoneme of cilia and flagella. *J. Theor. Biol.* 168:175–89
Lindemann C. 2003. Structural-functional relationships of the dynein, spokes, and central-pair projections predicted from an analysis of the forces acting within a flagellum. *Biophys. J.* 84:4115–26
Lindemann C. 2004. Testing the geometric clutch hypothesis. *Biol. Cell* 96:681–90
Lindemann C, Kanous K. 1995. Geometric clutch hypothesis of axonemal function: key issues and testable predictions. *Cell Motil. Cytoskelet.* 31:1-8
Mernone AV, Mazumdar JN, Lucas SK. 2002. A mathematical study of peristaltic transport of a Casson fluid. *Math. Comp. Model.* 35:895–912
Mitchell DR. 2003. Orientation of the central pair complex during flagellar bend formation in Chlamydomonas. *Cell Motil. Cytoskel.* 56:120–29
Mittal R, Iaccarino G. 2005. Immersed boundary methods. *Annu. Rev. Fluid Mech.* 37:239–61
Moore H, Dvorakova K, Jenkins N, Breed W. 2002. Exceptional sperm cooperation in the wood mouse. *Nature* 418:174–77
Murase M. 1992. *The Dynamics of Cellular Motility*. Chichester, UK: John Wiley
Omoto CK. 1991. Mechanochemical coupling in cilia. *Int. Rev. Cytol.* 131:255–92
Osada H, Tsunoda I, Matsuura M, Satoh K, Kanayama K, Nakayama Y. 1999. Investigation of ovum transport in the oviduct: the dynamics of oviductal fluids in domestic rabbits. *J. Int. Med. Res.* 27:176–80
Peskin CS. 1977. Numerical analysis of blood flow in the heart. *J. Comp. Phys.* 25:220
Peskin CS. 2002. The immersed boundary method. *Acta Numer.* 11:479–517
Peskin CS, McQueen DM. 1989. A three-dimensional computational model for blood flow in the heart I. *J. Comp. Phys.* 81:372–405
Peskin CS, McQueen DM. 1989. A three-dimensional computational model for blood flow in the heart II. *J. Comp. Phys.* 82:289
Phan-Thien N, Tran-Cong T, Ramia M. 1987. A boundary element analysis of flagellar propulsion. *J. Fluid Mech.* 184:533–49
Pozrikidis C. 1992. *Boundary Integral and Singularity Methods for Linearized Viscous Flow*. Cambridge, UK: Cambridge Univ. Press
Pozrikidis C. 1987. A study of peristaltic flow. *J. Fluid Mech.* 180:515–27
Rejniak K, Kliman H, Fauci L. 2004. A computational model of the mechanics of growth of the villous trophoblast bilayer. *Bull. Math. Biol.* 66:199–232

Rothschild L. 1963. Non-random distribution of bull spermatazoa in a drop of sperm suspension. *Nature* 198:1221–22
Scott MA. 2000. A glimpse at sperm function in vivo: sperm transport and epithelial interaction in the female reproductive tract. *Anim. Reprod. Sci.* 60:337–48
Shingyoji C, Higuchi H, Yoshimura M, Katayama E, Yanagida T. 1998. Dynein arms are oscillating force generators. *Nature* 393:711–14
Stauss C, Votta T, Suarez S. 1995. Sperm motility hyperactivation facilitates penetration of the hamster zona pellucida. *Biol. Reprod.* 53:1280–85
Suarez S. 1996. Hyperactivated motility in sperm. *J. Androl.* 17:331–35
Suarez S, DeMott RP. 1991. Functions of hyperactivated motility of sperm in the oviduct. *Arch. Biol. Med. Exp.* 24:331–37
Suarez S, Katz D, Owen D, Andrew J, Powell R. 1991. Evidence for the function of hyperactivated motility in sperm. *Biol. Reprod.* 44:375–81
Sun Y, Wan K, Roberts K, Bischof J, Nelson B. 2003. Mechanical property characterization of mouse zona pellucida. *IEEE Trans. Nanobiosci.* 2(4):279–86
Takabatake S, Ayukawa K, Mori A. 1988. Peristaltic pumping in circular cylindrical tubes: a numerical study of fluid transport and its efficiency. *J. Fluid Mech.* 193:267–83
Talbot P, Geiske C, Knoll M. 1999. Oocyte pickup by the mammalian oviduct. *Mol. Biol. Cell* 10:5–8
Talbot P, Shur BD, Myles DG. 2003. Cell adhesion and fertilization: steps in oocyte transport, sperm-zona pellucida interactions, and sperm-egg fusion. *Biol. Reprod.* 68:1–9
Tang D, Rankin S. 1993. Peristaltic motions of viscous flow with elastic free boundaries. *SIAM J. Sci. Comp.* 14:1300–19
Taylor GI. 1951. Analysis of the swimming of microscopic organisms. *Proc. R. Soc. London Ser. A* 209:447–61
Tollner T, Yudin A, Cherr G, Overstreet J. 2003. Real-time observations of individual macaque sperm undergoing tight binding and the acrosome reaction on the zona pellucida. *Biol. Reprod.* 68:664–72
Verdugo P, Lee W, Halbert S, Blandau R, Tam P. 1980. A stochastic model for oviductal egg transport. *Biophys. J.* 29:257–70
Williams M, Hill CJ, Scudamore I, Dunphy B, Cooke ID, Barratt C. 1993. Sperm numbers and distribution within the human Fallopian tube around ovulation. *Human Reprod.* 8:2019–26
Winet H, Bernstein GS, Head J. 1984. Observations on the response of human spermatazoa to gravity, boundaries and fluid shear. *J. Reprod. Fert.* 70:511–23
Witman GB. 1990. *Introduction to Cilia and Flagella*, *in Ciliary and Flagellar Membranes*, ed. RA Bloodgood. New York: Plenum
Woolley DM. 2003. Motility of spermatozoa at surfaces. *Reproduction* 126:259–70
Yanagimachi R. 1970. The movement of golden hamster spermatozoa before and after capacitation. *J. Reprod. Fert.* 23:193–96
Yaniv S, Elad D, Jaffa AJ, Eytan O. 2003. Biofluid aspects of embryo transfer. *Ann. Biomed. Eng.* 31:1255–62

Annual Review of
Fluid Mechanics

Volume 38, 2006

Contents